Photofragmentation of Phase-Transferred Gold Nanoparticles by Intense Pulsed Laser Light

Zhangquan Peng,[†] Thomas Walther,[‡] and Karl Kleinermanns*,[†]

Institute for Physical Chemistry, Heinrich-Heine-Universität Düsseldorf, 40225 Düsseldorf, and Center of Advanced European Studies and Research, Ludwig-Erhard-Allee 2, 53175 Bonn, Germany

Received: April 9, 2005; In Final Form: June 27, 2005

Gold nanoparticles with an average diameter of ∼20 nm were prepared in an aqueous solution by a wet chemistry method. The parent gold nanoparticles were then capped with a 4-aminothiophenol protecting layer and transferred into toluene by tuning the surface charge of the modified nanoparticles. Gold nanoparticles before and after phase transfer were subjected to photofragmentation by a pulsed 532 nm laser. The effects of solvent properties and surface chemistry on the photofragmentation of the gold nanoparticles have been investigated. Fast photofragmentation has been observed in the organic solvent in which the dielectric constant, heat capacity, and thermal conductivity are lower. The results suggest new approaches for the preparation of very small gold clusters from gold nanoparticles.

Introduction

During the past two decades, many research efforts have been focused on metal nanoparticles because of their unique size-dependent physical and chemical properties.[1] In this context it is significant to develop low-cost and effective methods for the preparation of nanoparticles with the desired size. Size-selective preparation of nanoparticles with diameters ranging from 1 to 100 nm can easily be achieved by using wet chemistry methods, where a metal salt is reduced by a reductant in the presence of protecting ligands.[2] One drawback of the wet chemistry method is the possible contamination from the reducing reagents or the protecting ligands used.

Recently, a physical method, i.e., laser ablation, has been used to prepare metal nanoparticles in solution.[3] This laser-based method is contaminant free, but the size distribution of the nanoparticles tends to be wide because aggregation of the ablated atoms and clusters is difficult to control. On the basis of laser ablation, a method called "laser-assisted size reduction" has been developed to fragment metal nanoparticles into smaller ones through their selective heating caused by resonant electronic excitation of the parent nanoparticles.[4] For example, the surface plasmon band of gold nanoparticles centered at 520 nm can be excited by an intense pulsed 532 nm laser, because its energy is in the vicinity of the absorption maximum of the gold nanoparticles. Several studies have been performed on laser-assisted size reduction of gold nanoparticles in solution using different lasers.[5] For instance, gold nanoparticles of 20 nm diameter can be selectively transformed into nanonetworks or smaller nanoparticles depending on the proper combination of the fluence of a 532 nm laser and the protecting ligand concentration.[6a] Gold nanorods can be thermally isomerized into spherical nanoparticles by a femtosecond laser,[6b] or fragmented into smaller nanoparticles by nanosecond laser irradiation.[6c] Gold flakes (0.1−0.2 μm thick and 10 μm in diameter) suspended in water can be fragmented using nanosecond 532 nm laser radiation to spherical submicroparticles first and subsequently to fine nanoparticles significantly less than 10 nm in diameter.[6d] Gold nanoparticle aggregates induced by adsorption of thiobarbituric acid[6e] or thionicotinamide[6f] can be dissociated and fragmented into isolated smaller nanoparticles using 532 nm laser irradiation.

To establish better size control in solution, it is necessary to elucidate the mechanism of how the shape of the nanoparticles changes and how photofragmentation proceeds. Some parameters that have important effects on the photophysical process of nanoparticles are the energy fluence, laser pulse width, and protecting ligands.[5,6a] While these effects are quite well studied, the influence of the solvent and the surface chemistry of the nanoparticles are largely unknown.[7] In this paper, we report the dependence of photofragmenation on the solvent, ligands, and surface chemistry of gold nanoparticles by using a phase-transfer procedure. Our ultimate goal is to obtain gold clusters with well-defined band gaps and semiconductor-like optical properties by using laser-based size reduction.[8] We prepared gold nanoparticles in water via $AuCl_4^-$ reduction by citrate. With this technique size control is straightforward.[2b] Then the gold nanoparticles were surface-capped with a 4-aminothiophenol (4-ATP) protecting layer, and successively transferred into toluene by tuning the surface charge of the modified nanoparticles.[9] The modified gold nanoparticles were then subjected to photofragmenation in water, toluene, and a toluene/methanol mixture by a pulsed 532 nm laser. The effect of the concentration of 4-ATP in the solution on the photofragmentation process has also been studied. Fast photofragmentation has been observed in the organic phase. Dielectric, heat capacity, and thermal conductivity properties of the solvents have been considered to explain the observed experimental results.

Experimental Section

Chemicals and Procedure. Gold(III) chloride trihydrate ($HAuCl_4 \cdot 3H_2O$; 99.9+%), sodium citrate dihydrate (99+%), 4-aminothiophenol (4-ATP, $HSC_6H_4NH_2$; 97%), toluene (99.8%), and methanol (99.5%) were purchased from Aldrich and were

* To whom correspondence should be addressed. Fax: +49-211-8115195. E-mail: kleinermanns@uni-duesseldorf.de.
[†] Heinrich-Heine-Universität Düsseldorf.
[‡] Center of Advanced European Studies and Research.

10.1021/jp051849a CCC: $30.25 © 2005 American Chemical Society
Published on Web 07/28/2005

used as received. Gold colloids were synthesized by addition of $AuHCl_4 \cdot 3H_2O$ (20 mg) to a refluxing, rapidly stirred solution of sodium citrate (60 mg) in water (250 mL), which was stirred under reflux for an additional 15 min before being allowed to cool.[2b] The obtained colloidal solution has a pH value of 4.7. The particle size and the size distribution were verified by optical absorbance spectroscopy and transmission electron microscopy. A 30 mL sample of an aqueous dispersion of gold nanoparticles was taken, to which 3 mL of 1 mM 4-ATP/1 mM HCl solution was slowly added. Then the pH of the solution was adjusted to 3 using dilute hydrochloric acid. Neither the 4-ATP addition nor the pH adjustment resulted in visible destabilization of the colloidal solution. A 30 mL sample of toluene was added to this solution, leading to the formation of a two-phase system. Vigorously stirring the mixture and slowly adjusting the pH of the water phase from 3 to 7 resulted in the transfer of gold nanoparticles from the aqueous to the organic phase, which can be seen from the red color upon the transfer from water to toluene. After completion of the phase transfer, the organic phase was separated and washed with copious water to remove the citrate in the toluene phase.

Instrumentation. Optical absorption spectra of the colloidal solution were recorded by using a Cary 300 UV/vis spectrophotometer operated at a resolution of 1 nm. The size and shape of the gold colloids were investigated with a LEO 922A TEM instrument operated at an accelerating voltage of 200 kV. The TEM samples were prepared by adding droplets of the colloidal solution of interest on carbon-coated copper grids (Cu-400CK, Pacific Grid-Tech) and allowing them to dry in air. Bright-field images were recorded at a nominal magnification of 80000×, which was calibrated to 2% precision. The particle sizes were determined by using successive gray level thresholding of the images, noise removal by image filtering, and particle erosion with the AnalySIS 3.2 software package. A pulsed Nd:YAG laser (Quanta Ray INDI series, Spectra Physics, Mountain View, CA) with a beam diameter of about 8 mm was used to irradiate the colloidal solution at a repetition rate of 10 Hz at 532 nm. The energy fluence per pulse is 130 mJ/cm^2 at a pulse length of 6 ns.

Results and Discussion

Phase Transfer of Aqueous Gold Nanoparticles into the Toluene Phase. The transfer of aqueous gold nanoparticles into nonpolar organic solvents requires hydrophobilization of the nanoparticle surface. Many strategies have been developed to accomplish phase transfer into organic solvents, which differ in the nature of the capping molecules employed to hydrophobilize the nanoparticles. Polymers,[10] alkylthiols,[11] alkylamines,[12] host−guest complexes,[13] and ionic surfactants[14] have been successfully used as reagents to transfer citrate-reduced and stabilized gold nanoparticles from the aqueous to the organic phase. In our case the phase-transfer reagents are 4-ATP molecules with two functional groups, namely, −SH and $-NH_2$. Thiol moieties can covalently bond to a gold surface, and amino moieties show pH-dependent protonation.[15] 4-ATP can readily dissolve in water at pH 3.0 because of the protonation of the amino moiety in an acidic environment, while upon adjustment of the pH of the solution to 7.0 a white precipitate is immediately observed, showing its poor solubility under neutral conditions. The solid curve in Figure 1 is the UV/vis spectrum recorded from the gold nanoparticles in water with dissolved 0.1 mM 4-ATP at pH 3.0. Compared with the spectrum of the parent colloidal solution,[6e] a red shift in the surface plasmon resonance from 520 to 526 nm along with a slight absorption decrease is

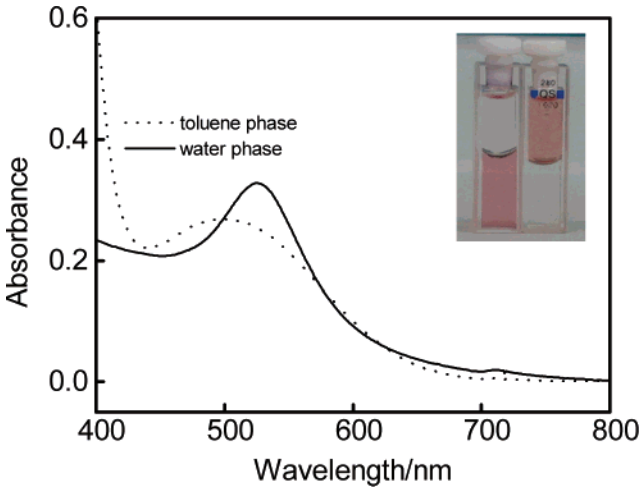

Figure 1. Optical absorption spectra of 4-ATP-capped gold nanoparticles before (solid curve) and after (dotted curve) phase transfer from water to toluene. The inset shows cuvettes before (left) and after (right) the phase-transfer procedure.

observed, indicating the capping of the gold nanoparticles via thiolate linkages.[16] By slowly varying the pH value of the water phase from 3.0 to 7.0 in the presence of toluene under vigorous stirring, the transfer of the surface-capped gold nanoparticles from water to toluene has been achieved. The dotted curve in Figure 1 is the UV/vis spectrum of the gold nanoparticles in toluene after phase transfer as described above. The surface plasmon resonance is broadened and shifted to the blue. The organic solution of the gold nanoparticles was very stable with no precipitation observed even 3 months after the phase-transfer procedure. The only difference between the particles before and after the phase transfer is the surface charge of the 4-ATP-capped nanoparticles. In water at pH ≈ 3.0 the amino moieties on the particle surface are protonated, which leads to a highly charged particle surface, while in toluene the charge density on the particle surface is much lower.

It is quite intriguing that the resonance absorbance of the gold nanoparticles shifts to higher frequencies in toluene. For isolated gold nanoparticles with spherical shape, the wavelength of the resonance absorbance maximum depends on the particle size, surface-adsorbed species, and the dielectric medium surrounding the particles.[17] The blue shift of the resonance absorbance can be attributed to a decrease of particle size or an increase of the refractive index of the medium.[10] Modifying the gold particle surface with strong ligands (for example, alkanethiols) has more complicated effects on the optical properties of the particles: (i) the formation of the Au−S bond will damp the collective oscillation of the conducting electrons to some extent, leading to a decrease in the absorbance intensity;[18] (ii) the existence of a thin organic layer with an increased refractive index will cause a red shift of the resonance absorbance;[2a] (iii) when the charges of the nanoparticles are changed by injecting or withdrawing electrons to or from the metal core, or by redox or acid−base reactions of the redox or ionizable moieties on the periphery of the nanoparticles, both the intensity and the shift of the resonance absorbance depend on the charge of the nanoparticles.[19] Note that, for alkylthiol-protected gold nanoparticles, the effect of the solvent refractive index is minor and the effective refractive index becomes that of the alkylthiol layer.[19b] We conclude that it is the difference in the surface charge of the nanoparticles in water and toluene that leads to the blue shift of the observed resonance absorbance. Similar results have also been reported by other groups. For instance, Tong et al.

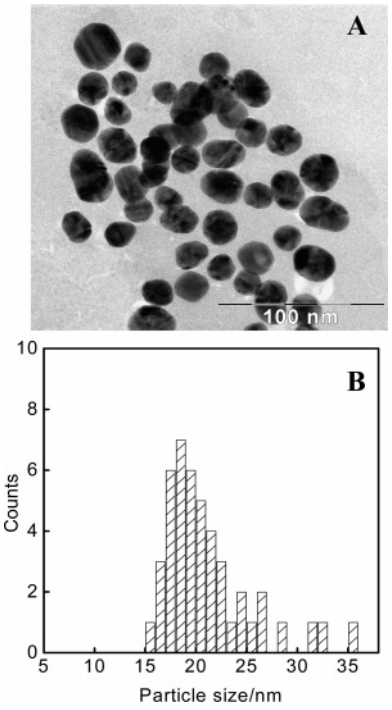

Figure 2. Electron micrograph and size distribution (21.3 ± 4.4 nm) of gold nanoparticles in water before phase transfer.

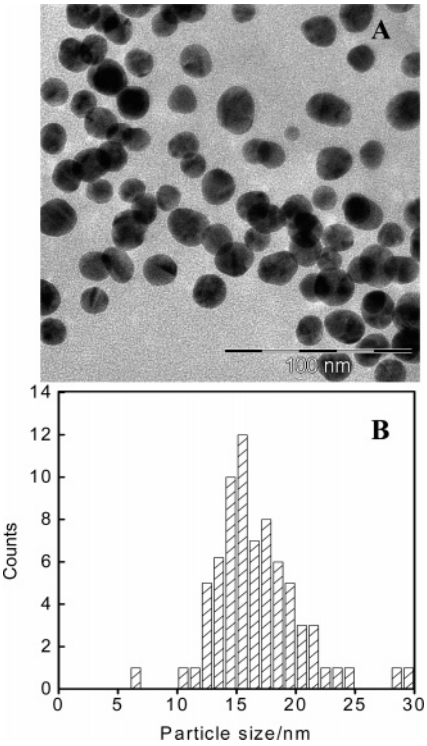

Figure 3. Electron micrograph and size distribution (17.2 ± 3.0 nm) of gold nanoparticles in toluene after phase transfer.

reported a blue shift of the resonance absorbance of 2 nm octylthiol-protected gold nanoparticles when electrons were injected into the gold core by using a quantized electrochemical double-layer charging method.[19d] Similarly, Mulvaney and co-workers reported a red shift of the resonance absorbance of 5.2 nm dodecanethiol-protected gold nanoparticles when electrons were withdrawn from the gold core.[19b] Upon oxidation of the ferrocene moieties on gold nanoparticles of 3−5 nm diameter, a red shift of the resonance absorbance has been observed.[19c] All these observations indicate that, besides the core charge, the surface charge of the particles has a significant effect on their optical absorbance. In summary, nanoparticles with negative or zero charge show a blue shift of the resonance absorbance compared to those with positive charge.

Our observations of a very small plasmon resonance absorption of the gold nanoparticles and a weak absorbance (between 200 and 300 nm) due to 4-ATP left in the aqueous phase demonstrate that an almost complete phase transfer of both the Au nanoparticles and the 4-ATP molecules had occurred. A picture of the cuvettes containing the biphasic mixture before and after phase transfer is shown in the inset of Figure 1. Representative TEM images together with size distributions of the gold nanoparticles in the water (Figure 2) and toluene phase (Figure 3) reveal that the particles are spherical in shape and reasonably uniform in size. Before and after phase transfer there is no obvious change in particle size and shape, suggesting that the etching of the nanoparticles by thiols is a kinetically slow process at room temperature.

Laser-Induced Photofragmentation of 4-ATP-Capped Gold Nanoparticles in Water and Toluene. Upon laser irradiation at 532 nm, a gold nanoparticle is able to absorb many photons during a single laser pulse.[4c] Gold atoms and clusters will be released from the excited parent nanoparticles by Coulombic[20] or thermal explosion mechanisms.[4b] By using gold nanoparticles in water and toluene with the same size and surface chemistry, it is possible to investigate specifically the influence of the dielectric properties of the solvent and the identity and amount of the protecting ligands on the photofragmentation

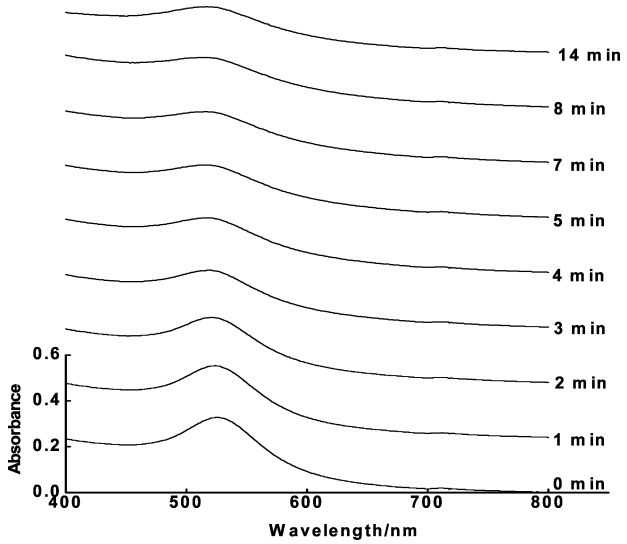

Figure 4. Optical absorption spectra of 4-ATP-capped nanoparticles in water at different laser irradiation times at 532 nm.

process. Figure 4 shows the optical absorption spectra of the modified gold nanoparticles in water irradiated by a pulsed laser at 532 nm and 130 mJ/cm^2 for different irradiation times. With increasing irradiation time, the absorption intensity around 526 nm decreases and the width of the absorbance peak is broadened. Also, a slight blue shift of the resonance absorbance from 526 to 518 nm is observed. This spectral change indicates that the nanoparticles are shattered by the laser irradiation so that the average diameter of the nanoparticles is reduced.[21] Similar results have also been observed in our previous work, where gold nanoparticle aggregates induced by surface acid−base reaction were subjected to 532 nm laser irradiation.[6e] Upon laser irradiation, the aggregates dissociated and the isolated nanoparticles were fragmented into smaller ones. It is also possible that some tiny molecular gold clusters (<1 nm in diameter)

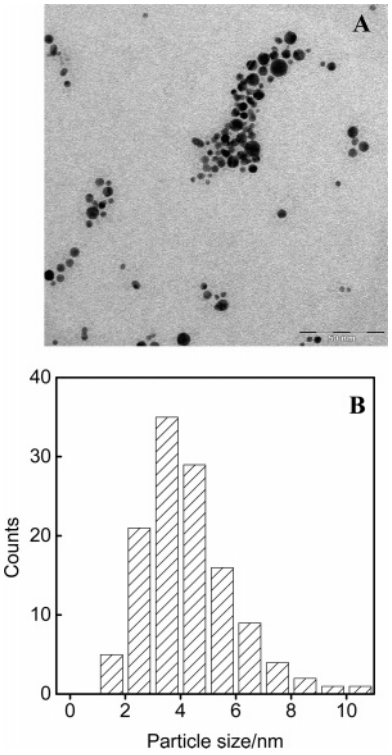

Figure 5. Electron micrograph and size distribution (4.3 ± 1.6 nm) of gold nanoparticles in water after 8 min of laser irradiation at 532 nm.

without plasmon absorption ("colorless", i.e., invisible in the visible spectral region) have been produced during the irradiation process, since the intensity of the resonance absorption after laser irradiation is always lower than that of the parent colloidal solution.

To assess the morphological changes caused by laser irradiation, we again studied the photoproducts by TEM. One representative TEM micrograph (Figure 5A) of 4-ATP-capped gold nanoparticles in water after 8 min of laser irradiation shows the appearance of photofragments of smaller gold nanoparticles. The TEM images support the hypothesis that the parent nanoparticles undergo fragmentation and thereby produce smaller nanoparticles. It has been reported that the released gold atoms have a strong tendency to rapidly aggregate into small gold clusters on a nanosecond time scale.[22] Single gold atoms or small gold nanoparticles could also diffuse to and aggregate at the surface of preexisting larger particles.[4e] Gold clusters begin to contribute to the optical absorption at around 520 nm as they grow into nanosized particles by aggregation and attachment to other nanoparticles. Under certain conditions very large nanoparticle aggregates (lines and networks with a size of tens of nanometers) and larger nanoparticles can be formed by interparticle fusion.[6a] In our case, however, we did not observe any aggregation and interparticle fusion even under long-term (18 min) laser irradiation, which can be attributed to the excess amount of 4-ATP protecting ligands that can readily adsorb on newly formed fresh gold surfaces.[23]

In toluene much more efficient photofragmentation than in water has been observed for the 4-ATP-capped gold nanoparticles. Even irradiation for only 5 min irreversibly bleaches the resonance absorbance around 510 nm (Figure 6) as observed from the color change of the toluene phase from red to almost colorless (Figure 6 inset). It is obvious that in toluene the parent gold nanoparticles can be easily photofragmentated into tiny gold clusters by laser irradiation. TEM examination of the

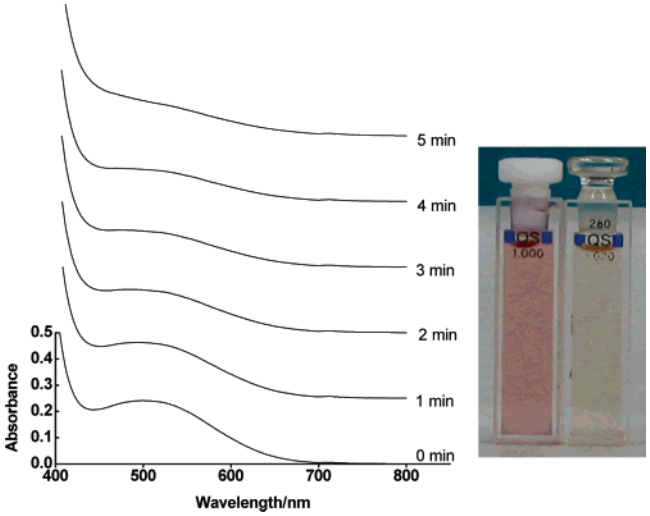

Figure 6. Optical absorption spectra of 4-ATP-capped gold nanoparticles in toluene at different irradiation times at 532 nm. The right inset shows a photograph of the samples at 0 and 5 min of irradiation.

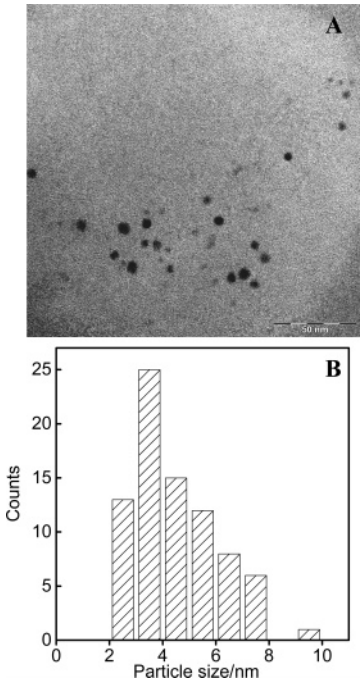

Figure 7. Electron micrograph and size distribution (4.5 ± 1.7 nm) of residual gold nanoparticles in toluene after 3 min of laser irradiation at 532 nm. Only very few of these medium-sized gold photofragments have been found across the whole copper grid. Most of the photofragments are too small to be visible in the TEM image; see the text.

photoproducts showed that it is very difficult to find well-defined nanoparticles in the sample obtained from the laser-irradiated toluene solution. Probably, the size of most of the photoproducts is smaller than the detection limit in bright-field TEM, which typically lies somewhere between 1 and 2 nm for a flat carbon support grid and will only be lower in either energy-filtered TEM[24] or annular dark-field STEM.[25] Only very few smaller residual gold nanoparticles have been found across the whole copper grid (Figure 7). From the dramatic decrease in absorbance near 510 nm, we can infer that most of the photofragments are so small that they lose their plasmon absorbance in the visible region. The excess amount of 4-ATP in toluene suppresses the aggregation of smaller photofragments into larger nanoparticles.[6a] Furthermore, there has been no change in the

SCHEME 1: Photofragmentation of 4-ATP-Capped Gold Nanoparticles in the Presence of Excess 4-ATP Protecting Ligands

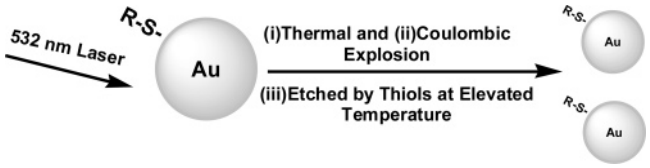

absorbance spectra for months, indicating that the photofragments released into the solution must be very stable.

By comparing the photofragmentation of gold nanoparticles in water and toluene, we obtain some insight into the mechanism of the photofragmentation process (Scheme 1). There are two possible pathways for the photofragmentation process, namely, thermal or charge-induced explosion (by Coulomb repulsion of charges with the same sign). Upon irradiation with an intense pulsed laser at 532 nm (130 mJ/pulse), a parent nanoparticle in the colloidal solution will experience multiphoton absorption during a single laser pulse, and the nanoparticle will be heated to its boiling point in a few picoseconds via electron−phonon interactions.[5] These hot gold nanoparticles fragment into smaller nanoparticles by releasing atoms and clusters. Besides, gold nanoparticles will be efficiently ionized, and the charge density produced may be sufficient to cause explosive repulsion.[21] In our water and toluene samples the initial gold nanoparticles have the same size and surface chemistry; the main difference is the dielectric medium surrounding the gold nanoparticles. Both the Coulombic and thermal fragmentation mechanisms depend on solvent properties including the dielectric constant ($\epsilon_{water} = 80.1$, $\epsilon_{toluene} = 2.38$), the heat capacity ($C_{water} = 4.18$ J g^{-1} K^{-1}, $C_{toluene} = 1.70$ J g^{-1} K^{-1}), and the thermal conductivity ($\Lambda_{water} = 0.607$ W m^{-1} K^{-1}, $\Lambda_{toluene} = 0.131$ W m^{-1} K^{-1}) of the corresponding solvent. From the viewpoint of the Coulombic mechanism, we should observe more efficient photofragmentation in a medium with a lower dielectric constant because of its poor ability to screen the charges and to stabilize the charged species. From the viewpoint of a purely thermal explosion mechanism, lower heat capacity and thermal conductivity are favorable for the fragmentation.[26] Besides the Coulumbic and the thermal mechanisms for the size reduction of gold nanoparticles, there might be another possibility from the surface chemistry of gold when organic thiols adsorb, leading to the formation of a Au−S bond. The formation of a Au−S bond causes the etching of the gold surface,[27] and the extent of etching is temperature dependent. Recently, we observed that a Au(111) substrate can be more severely etched by organic thiols at higher temperature than at room temperature; see the Supporting Information. Similarly, Scherer et al.[28] reported that Au nanoparticles in an organic solvent can be converted into atomic Au clusters in the presence of concentrated organic thiols under high-temperature conditions (at ∼300 °C). We also think that the etching of gold nanoparticles depends on the nature of the solvent because the temperature gradient around the laser-excited gold nanoparticles is solvent dependent. On the basis of the experimental results, we can conclude that the size reduction process is more favored in toluene than in water so it is possible to obtain small gold clusters by laser irradiation due to the lower dielectric, heat capacity, and thermal conductivity properties of toluene compared to water.

Effects of Solvent Properties and the Concentration of the Protecting Ligands. To further verify the effects of solvent properties on the photofragmentation, we performed the fragmentation experiments in a 1:1 mixture of toluene and methanol

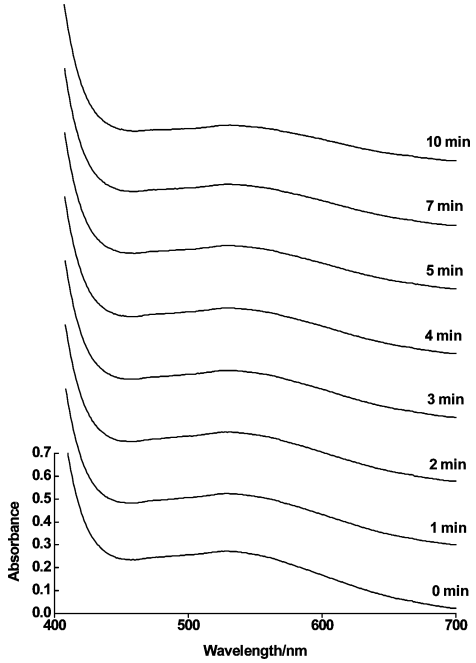

Figure 8. Optical absorption spectra of 4-ATP-capped nanoparticles in a 1:1 mixture of toluene and methanol at different laser irradiation times at 532 nm.

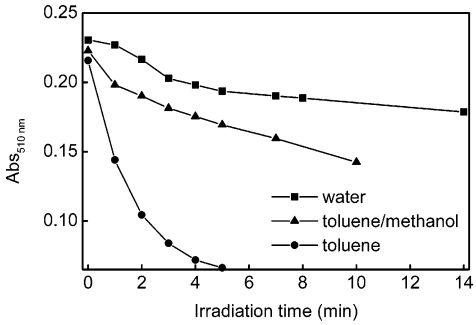

Figure 9. Absorbance of 4-ATP-capped nanoparticles at 510 nm as a function of the irradiation time in different solvents.

($\epsilon = 33.0$, $C = 2.53$ J g^{-1} K^{-1}, and $\Lambda = 0.200$ W m^{-1} K^{-1}) with the same concentration of gold nanoparticles. Since the dielectric constant, heat capacity, and thermal conductivity of the mixture must lie between those of toluene and methanol, we expect that an intermediate rate of photofragmentaion of the gold nanoparticles should be observed. Figure 8 shows the optical absorption spectrum upon fragmentation of the gold nanoparticles in the mixture. Compared with the results in Figures 4 and 6, an intermediate photofragmentation efficiency is indeed observed (see Figure 9), as expected.

By taking fragmentation and growth mechanisms of gold nanoparticles into account,[4e] we can obtain small gold clusters by optimizing the concentration of 4-ATP. As shown in Figure 10 compared to Figure 6 (see, for example, the curves for 3 min of irradiation time), the absorbance of gold nanoparticles at around 510 nm decreases more rapidly in the 1 mM 4-ATP solution than in the 0.1 mM 4-ATP solution. This allows us to conclude that the gold clusters formed by laser irradiation in a concentrated 4-ATP solution have a reduced tendency to aggregate or attach to other nanoparticles. The absence of aggregation and particle growth can be attributed to the tight coating with 4-ATP. Gold clusters are readily coated by a monolayer of 4-ATP directly after their formation, and 4-ATP forms a steric barrier for the clusters to avoid aggregation. As

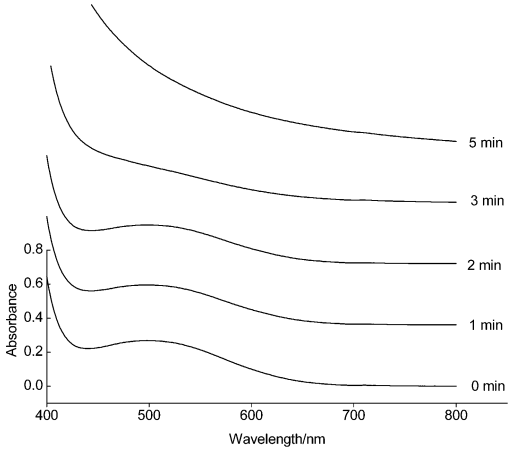

Figure 10. Optical absorption spectra of 4-ATP-capped nanoparticles in toluene at a higher concentration of 4-ATP ligands (~1 mM) at different laser irradiation times at 532 nm.

the 4-ATP concentration increases, the rate of the capping of the photoproducts also increases, and hence, the rate of collisions between bare photofragments decreases.

Conclusions

Laser-assisted size reduction of phase-transferred gold nanoparticles with an average diameter of ~20 nm was performed. Some parameters involved in the photofragmentation process including solvent properties and the surface chemistry of the gold nanoparticles have been investigated by using optical absorption spectroscopy and transmission electron microscopy. Solvents with lower dielectric constant, heat capacity, and thermal conductivity have been shown to be favorable for photofragmentation of gold nanoparticles. The laser-assisted size reduction is a promising technique for the preparation of small gold clusters with molecular or semiconductor-like optical properties.

Acknowledgment. Z.P. acknowledges the support by the Alexander von Humboldt Foundation. Z.P. thanks Xiaohu Qu (Changchun Institute of Applied Chemistry) for the acquisition of the STM images.

Supporting Information Available: STM images of a Au(111) facet obtained by dipping the precleaned Au(111) substrate into a ~1 mM ethanolic solution of $SH(CH_2)_{11}CH_3$ at room temperature and at elevated temperature. This material is available free of charge via the Internet at http://pubs.acs.org.

References and Notes

(1) (a) Daniel, M.-C.; Astruc, D. *Chem. Rev.* **2004**, *104*, 293. (b) Thomas, K. G.; Kamat, P. V. *Acc. Chem. Res.* **2003**, *36*, 888. (c) Sastry, M.; Rao, M.; Ganesh, K. N. *Acc. Chem. Res.* **2002**, *35*, 847. (d) Crooks, R. M.; Zhao, M.; Sun, L.; Chechik, V.; Yeung, L. K. *Acc. Chem. Res.* **2001**, *34*, 181.

(2) (a) Templeton, A. C.; Wuelfing, W. P.; Murray, R. W. *Acc. Chem. Res.* **2000**, *33*, 27. (b) Shipway, A. N.; Katz, E.; Willner, I. *ChemPhysChem* **2000**, *1*, 18.

(3) (a) Fojtik, A.; Henglein, A. *Ber. Bunsen-Ges. Phys. Chem.* **1993**, *97*, 252. (b) Sibbald, M. S.; Chumanov, G.; Cotton, T. M. *J. Phys. Chem.* **1996**, *100*, 4672. (c) Yeh, M.-S.; Yang, Y.-S.; Lee, Y.-P.; Lee, H.-F.; Yeh, Y.-H.; Yeh, C.-S. *J. Phys. Chem. B* **1999**, *103*, 6851. (d) Mafune, F.; Kohno, J.; Takeda, Y.; Kondow, T.; Sawabe, H. *J. Phys. Chem. B* **2000**, *104*, 8333. (e) Mafune, F.; Kohno, J.; Takeda, Y.; Kondow, T.; Sawabe, H. *J. Phys. Chem. B* **2000**, *104*, 9111. (f) Mafune, F.; Kohno, J.; Takeda, Y.; Kondow, T.; Sawabe, H. *J. Phys. Chem. B* **2001**, *105*, 5114. (j) Brause, R.; Möltgen, H.; Kleinermanns, K. *Appl. Phys. B* **2002**, *75*, 711.

(4) (a) Kurita, H.; Takami, A.; Koda, S. *Appl. Phys. Lett.* **1998**, *72*, 789. (b) Takami, A.; Kurita, H.; Koda, S. *J. Phys. Chem. B* **1999**, *103*, 1226. (c) Mafune, F.; Kohno, J.; Takeda, Y.; Kondow, T. *J. Phys. Chem. B* **2001**, *105*, 9050. (d) Mafune, F.; Kohno, J.; Takeda, Y.; Kondow, T. *J. Phys. Chem. B* **2002**, *106*, 7575. (e) Mafune, F.; Kohno, J.; Takeda, Y.; Kondow, T. *J. Phys. Chem. B* **2002**, *106*, 8555.

(5) (a) El-Sayed, M. A. *Acc. Chem. Res.* **2001**, *34*, 257. (b) Kamat, P. V. *J. Phys. Chem. B* **2002**, *106*, 7729.

(6) (a) Mafune, F.; Kohno, J.; Takeda, Y.; Kondow, T. *J. Phys. Chem. B* **2003**, *107*, 12589. (b) Link, S.; Burda, C.; Nikoobakht, B.; El-Sayed, M. A. *J. Phys. Chem. B* **2000**, *104*, 6152. (c) Link, S.; Burda, C.; Mohamed, M. B.; Nikoobakht, B.; El-Sayed, M. A. *J. Phys. Chem. A* **1999**, *103*, 1165. (d) Kawasaki, M.; Masuda, K. *J. Phys. Chem. B* **2005**, *109*, 9379. (e) Peng, Z.; Walther, T.; Kleinermanns, K. *Langmuir* **2005**, *21*, 4249. (f) Fujiwara, H.; Yanagida, S.; Kamat, P. V. *J. Phys. Chem. B* **1999**, *103*, 2589.

(7) Ah, C. S.; Han, H. S.; Kim, K.; Jang, D.-J. *Pure Appl. Chem.* **2000**, *72*, 91.

(8) (a) Zhang, J.; Whitesell, J. K.; Fox, M. A. *J. Phys. Chem. B* **2003**, *107*, 6051. (b) Zheng, J.; Petty, J. T.; Dickson, R. M. *J. Am. Chem. Soc.* **2003**, *125*, 7780. (c) Wang, G.; Huang, T.; Murray, R. W.; Menard, L.; Nuzzo, R. G. *J. Am. Chem. Soc.* **2005**, *127*, 812.

(9) Isrealachvili, J. *Intermolecular and Surface Forces*, 2nd ed.; Academic Press: San Diego, CA, 1992.

(10) Underwood, S.; Mulvaney, P. *Langmuir* **1994**, *10*, 3427.

(11) (a) Sarathy, K. V.; Kulkarni, G. U.; Rao, C. N. R. *Chem. Commun.* **1997**, 537. (b) Sarathy, K. V.; Raina, G.; Yadav, R. T.; Kulkarni, G. U.; Rao, C. N. R. *J. Phys. Chem. B* **1997**, *101*, 9876. (c) Peng, Z.; Qu, X.; Dong, S. *Langmuir* **2004**, *20*, 5. (d) Peng, Z.; Wang, E.; Dong, S. *Electrochem. Commun.* **2002**, *4*, 210.

(12) (a) Leff, D. V.; Brandt, L.; Heath, J. R. *Langmuir* **1996**, *12*, 4723. (b) Sastry, M.; Kumar, A.; Mukherjee, P. *Colloids Surf., A* **2001**, *181*, 255.

(13) (a) Lala, N.; Lalbegi, S. P.; Adyanthaya, S. D.; Sastry, M. *Langmuir* **2001**, *17*, 3766. (b) Liu, J.; Xu, R.; Kaifer, A. E. *Langmuir* **1998**, *14*, 7337.

(14) (a) Chen, S.; Yao, H.; Kimura, K. *Langmuir* **2001**, *17*, 733. (b) Cheng, W.; Wang, E. *J. Phys. Chem. B* **2004**, *108*, 24.

(15) Bryant, M. A.; Crooks, R. M. *Langmuir* **1993**, *9*, 385.

(16) Mulvaney, P. *Langmuir* **1996**, *12*, 788.

(17) *Metal Nanoparticles: Synthesis, Characterization and Applications*; Feldheim, D. L., Colby, A. F., Jr., Eds.; Marcel Dekker: New York, 2002.

(18) Mulvaney, P. In *Nanoscale Materials in Chemistry*, Klabunde, K. J. Ed.; John Wiley & Sons: New York, 2001; Chapter 5.

(19) (a) Johnson, S. R.; Evans, S. D.; Brydson, R. *Langmuir* **1998**, *14*, 6639. (b) Templeton, A. C.; Pietron, J. J.; Murray, R. W.; Mulvaney, P. *J. Phys. Chem. B* **2000**, *104*, 564. (c) Qu, X.; Peng, Z.; Jiang, X.; Dong, S. *Langmuir* **2004**, *20*, 2519. (d) Lica, G. C.; Zelakiewicz, B. S.; Constantinescu, M.; Tong, Y. Y. *J. Phys. Chem. B* **2004**, *108*, 19896.

(20) (a) Näher, U.; Bjornholm, S.; Fraundorf, S.; Garcias, F.; Guet, C. *Phys. Rep.* **1997**, *285*, 245. (b) Last, I.; Schek, I.; Jortner. J. *J. Chem. Phys.* **1997**, *107*, 6685. (c) Last, I.; Jortner, J. *Phys. Rev. Lett.* **2001**, *87*, 033401.

(21) (a) Kamat, P. V.; Flumiani, M.; Hartland, G. V. *J. Phys. Chem. B* **1998**, *102*, 3123.

(22) Dawson, A.; Kamat, P. V. *J. Phys. Chem. B* **2001**, *105*, 960.

(23) (a) Sharma, J.; Mahima, S.; Kakade, B. A.; Pasricha, R.; Mandale, A. B.; Vijayamohanan, K. *J. Phys. Chem. B* **2004**, *108*, 13280. (b) Raj, C. R.; Kitamura, F.; Ohsaka, T. *Langmuir* **2001**, *17*, 7378. (c) Lukkari, J.; Kleemola, K.; Meretoja, M.; Ollonqvist, T.; Kankare, J. *Langmuir* **1998**, *14*, 1705.

(24) Walther, T.; Mader, W. *Proc. Electron Microsc. Anal. Group Conf. (EMAG-99, Sheffield), Inst. Phys. Conf. Ser.* **1999**, *161*, 243.

(25) (a) Creve, A. V.; Wall, J.; Langmore, J. *Science* **1970**, *168*, 1338. (b) Walther, T. *Proc. Eur. Microsc. Congr. (EMC2004, Antwerp)* **2004**, *2*, 119.

(26) Ge, Z.; Kang, Y.; Taton, T. A.; Braun, P. V.; Cahill, D. G. *Nano Lett.* **2005**, 5, 531.

(27) Sondag-Huethorst, J. A. M.; Schönenberger, C.; Fokkink, L. G. J. *J. Phys. Chem.* **1994**, *98*, 6826.

(28) Jin, R.; Egusa, S.; Scherer, N. F. *J. Am. Chem. Soc.* **2004**, *126*, 9900.